ASIAN JOURNAL OF PHARMACEUTICAL SCIENCES 12 (2017) 172–178

Available online at www.sciencedirect.com

ScienceDirect

journal homepage: www.elsevier.com/locate/ajps

Original Research Paper

Molecularly imprinted nanoparticles and their releasing properties, bio-distribution as drug carriers

Yongyan Zhu [a,1], Ling Yang [b,1], Dandan Huang [a], Quanhong Zhu [a,*]

[a] School of Traditional Chinese Medicine, Southern Medical University, Guangzhou 510515, China
[b] Department of Pharmacy, Nanfang Hospital, Southern Medical University, Guangzhou 510515, China

ARTICLE INFO

Article history:
Received 23 February 2016
Received in revised form 4 August 2016
Accepted 30 August 2016
Available online 20 September 2016

Keywords:
Molecular imprinted nanoparticles
Vinblastine
Drug carrier
Sustained release
Liver targeting

ABSTRACT

Molecular imprinted nanoparticles (MINPs) can memorize the shape and functional group positions complementary to template, which account for the large drug loading capacity and slow drug release behavior as drug carriers. We synthesized MINPs via precipitation polymerization with vinblastine (VBL) as a model drug, and investigated the drug loading, releasing property *in vitro* and bio-distribution *in vivo*. The obtained MINPs, from 300 to 450 nm, had smooth surface and favorable dispersibility. The entrapment efficacy and drug loading capacity of VBL loaded MINPs (MINPs-VBL) were 83.25% and 8.72% respectively. In PBS (pH7.4), MINPs-VBL showed sustained release behavior. The cumulative release percentage reached about 70% during 216 h and no burst release was observed. The releasing behavior of MINPs-VBL *in vitro* conformed to the first-order kinetics model. MINPs-VBL and commercially available vinblastine sulfate injection (VBL injection) were injected via tail vein of SD rats respectively to investigate the bio-distribution. MINPs-VBL group showed higher concentration of VBL in tissues and serum than VBL injection group after 60 min, and the drug level in liver was the highest. MINPs-VBL exhibited liver targeting trend to some extent, which was based on the evaluation of drug targeting index (DTI) and drug selecting index (DSI).

1. Introduction

The cavities in molecular imprinted polymers, complementary in shape, size and even chemical functionality to the template molecule, can recognize and absorb the template molecules with antibody-like affinities and selectivities [1]. The recognition and absorption mechanism is mainly governed by the combination of various non-covalent interactions, such as hydrogen bonds, ionic bonds, hydrophobic effect and van der Waals interactions between different functional groups of the MIPs and template molecule [2,3]. When the drug molecule is

* *Corresponding author.* School of Traditional Chinese Medicine, Southern Medical University, 1838 North Guangzhou Avenue, Guangzhou 510515, China. Fax: +86 20 6164 8770.
E-mail address: zqh@smu.edu.cn (Q. Zhu).
[1] The authors contributed equally to this work.
Peer review under responsibility of Shenyang Pharmaceutical University.
http://dx.doi.org/10.1016/j.ajps.2016.08.008

used as a template, the interactions between the MIPs and drug are very different from that of regular drug carriers, like embedding, or physical absorption, which are beneficial to the loading capacity and sustained release [2,4]. Asadi E. [5] reported that the loading of cyproterone in the imprinted polymers was significantly increased with respect to the non-imprinted polymers and it was attributed to the interactions between the functional groups of cyproterone and the carboxyl groups of polymer at the imprinted cavities. Furthermore, the sustained release of MIPs to drugs has also been confirmed by a wealth of cases. Abdouss [6] founded that the MIPs released citalopram more slowly than the non-imprinted polymers because of the non-covalent bindings. In addition, MIPs can also release the imprinted enantiomer with a slower rate than the opposite enantiomer when the racemic drug was loaded on the S-propranolol imprinted polymers [7].

Vinca alkaloids are a group of anti-mitotic and anti-microtubule alkaloid agents originally derived from the periwinkle plant *Catharanthusroseus*. Vinblastine (VBL) is one kind of Vinca alkaloids commonly used to treat Hodgkin's lymphoma, non-small cell lung cancer, bladder cancer, brain cancer, testicular cancer, and etc. But the narrow therapeutic window and severe dose-limiting, hematological toxicity, including leucopenia, myelosuppression and anemia, have always restricted its clinical application [8,9]. Nanoparticles, which have sustained release and targeting effect, maybe be an effective way to improve the dilemma. It was recently reported that vinblastine sulfate (VBL) was loaded in egg sphingomyelin/cholesterol liposome and achieved sustained release [10]. The poly(caprolactone) grafted dextran copolymeric nanoparticles loaded with vinblastine could not only sustain release *in-vitro* but could also enhance cellular uptake of NPs to increase the mortality of cancer cells and reduce the toxicity to normal cells [11].

In this paper, VBL imprinted nanoparticles were synthesized through precipitation polymerization, and the properties as a drug carrier for VBL were evaluated by drug loading and releasing *in vitro*. In addition, the effects of the carrier on VBL distribution *in vivo* were also investigated.

2. Materials and methods

2.1. Materials

Vinblastine sulfate (VBL) was purchased from Yueyang Biomedical Science and Technology Co., Ltd (Hainan, China), Batch No. 20090505; Methacrylate (MAA) was obtained from Yongda Reagent Center (Tianjin, China); Trimethylolpropane trimethacrylate (TRIM) was purchased from Sigma (America); Azobisisobutyronitrile (AIBN) was obtained from Sihewei Chemical Reagent Limited Company (Shanghai, China); Vinblastine sulfate for injection was from Shengtai Pharmaceutical Co., Ltd. (Shanxi province, China), Batch No. 20090422; Acetonitrile (HPLC grade) was purchased from Merck (Germany); Methanol and acetic acid was from Guangzhou Chemical Reagent Factory (Guangzhou, China).

SD rats (male or female, 200 ± 20 g) were from Experimental Animal Center of Southern Medical University (Guangzhou, China), No. SCXK Yue 2006-0015).

Table 1 – The effect of independent variables on dependent variable.

Entry	Independent variables				Dependent variables
	X_1 (MAA, mmol)	X_2 (TRIM, mmol)	X_3 (MeCN, ml)	X_4 (T, °C)	Y (Entrapment efficacy, %)
1	0.2	0.6	20	50	23.65 ± 1.31
2	0.3	1.2	30	60	9.90 ± 0.24
3	0.4	1.8	15	45	13.05 ± 0.47
4	0.5	0.2	25	60	76.60 ± 2.06
5	0.6	0.8	35	45	48.95 ± 2.89
6	0.7	1.4	15	55	23.15 ± 2.13
7	0.8	2.0	25	40	32.15 ± 3.73
8	0.9	0.4	35	55	57.40 ± 1.38
9	1.0	1.0	20	40	19.70 ± 0.13
10	1.1	1.6	30	50	29.45 ± 1.56

2.2. Preparation of MINPs via precipitation polymerization

The vinblastine imprinted nanoparticles were prepared from a reagent mixture obtained by mixing of VBL and MAA in acetonitrile according to Table 1. The solution was oscillated (CHY-2, Fuhua Instruments Co., Ltd, Jiangsu, China) for 30 min to prearrange template (VBL) and monomer (MAA). TRIM and AIBN (15 mg) were then added to the solution, and the mixture was sonicated in ultrasonic bath (KH-100DE, Kunshan Hechuang Ultrasound Instruments Co., Ltd, Jiangsu, China). Then it was purged for 5 min with N_2 and sealed. The polymerization was induced in a preheated water bath (HH-HS, Nanyang Instruments Co., Ltd, Shanghai, China) at 60 °C with shaking for 24 h. The polymeric particles were collected by centrifugation (TGL-168, Anting Scientific Instrument Factory, Shanghai, China) at 10,000 rpm for 5 min, and then extracted with methanol-glacial acetic acid (9:1, v/v) until no VBL could be detected in the washing solvent by UV Spectrophotometer (HP-8453, Agilent, USA) at 269 nm. The obtained imprinted nanoparticles were washed with methanol to remove the residual acetic acid, and then dried at 40 °C under vacuum for 24 h (ZK-82A, Shanghai Experimental Instrument Factory, Shanghai, China) to get MINPs.

2.3. Characterization of MINPs

The morphology of MINPs was observed by scan electron microscopy (SEM) (HITACHI S-3000 SEM, Japan). The polymer particles were coated with gold by sputtering prior to the SEM measurement. The particle size of MINPs was measured by a Malvern Zetasizer Nano ZS analyzer (Malvern Instruments Ltd, Malvern, UK) after being re-suspended in ultrapure water and diluted to appropriate concentration.

2.4. Preparation of MINPs-VBL

The drug loaded nanoparticles were prepared via dynamic adsorption. 40 mg of MINPs were immersed in 4 ml of vinblastine acetonitrile solution (1.25 mmol/l) and oscillated for 4 h at ambient temperature away from light. After centrifuged at 10,000 rpm for 5 min, the VBL loaded MINPs (MINPs-VBL) were collected and dried at 40 °C in a vacuum for 24 h. And the

supernatant was collected simultaneously to determine the amount of VBL bound to the nanoparticles.

2.5. *Determination of entrapment efficiency and drug loading capacity*

The content of VBL in the collected supernatant was determined by UV spectrophotometer at 269 nm. The amount of VBL bound to the nanoparticles was calculated by subtracting the amount of VBL in the supernatant from the initial. And the entrapment efficiency and drug loading capacity of the MINPs were calculated as the following equations:

$$\text{Entrapment efficiency (\%)} = \frac{\text{The amount of VLB bound to MINPs}}{\text{The initial amount of VLB}} \times 100\% \quad (1)$$

$$\text{Drug loading capacity (\%)} = \frac{\text{The amount of VLB bound to MINPs}}{\text{The amount of MINPs} + \text{The amount of VLB bound to MINPs}} \times 100\% \quad (2)$$

2.6. In vitro *drug release study*

40 mg of MINPs-VBL in 8 ml of PBS (pH 7.4) were placed in a centrifuge tube. The tube was oscillated in a water bath shaker (Incubator shakers KYC-2102C, Shanghai Shengke Science Instrument Equipment Co., LTD, Shanghai, China) at 60 rpm at 37 °C. At predetermined time intervals, a certain volume of dissolution medium was withdrawn, and at the meantime, the same volume of fresh release medium at 37 °C was complemented. The sample solution was centrifuged at 10,000 rpm for 5 min, and the concentration of VBL in the supernatant was analyzed by UV spectrophotometer at 269 nm. This process would be repeated until the absorbance of VBL was constant. The cumulative release percentage was calculated as the following equation:

$$\text{Cumulative release percentage (\%)} = \frac{C_n \times V_1 + \sum (C_{n-1} \times V_{n-1})}{M} \times 100\% \quad (3)$$

Here, C represents the concentration of free VBL in the supernatant; V is the volume of sample solution; V_1 is the total volume of release medium, and M is the amount of VBL in MINPs-VBL (the amount of VBL in MINPs-VBL is equal to the mass of MINPs-VBL multiplied by drug loading capacity).

The in vitro release behavior was plotted and fitted using different release dynamic models, including zero-order dynamic model, first order dynamic model, Higuchi equation and Retger–Peppas equation. The fitting degree of the models was evaluated with "r" and "AIC", which indicates a good coherence with real data.

(AIC = N*lnRe + P, "N" represents the number of experimental data, "P" is the model parameters). (Re = ∑Wi(Qexperiment – Qpattern)^2, "Wi" stands for Weight, equals to 1.)

2.7. *Bio-distribution study*

12 SD rats were fasted for 12 h with water ad libitum and randomly divided into two groups. Group 1, an experimental group, was injected with MINPs-VBL in saline solution at a dose of 5 mg/kg (calculated by VBL) via tail vein. Group 2 was administrated with the same dosage of commercially available vinblastine sulfate injection (VBL injection) as a control group. After 60 min, 6 ml of blood samples of groups 1 and 2 were collected respectively through the abdominal veins and immediately centrifuged at 10,000 rpm for 10 min, and the supernatant serum was stored at –20 °C until HPLC analysis. The rats were sacrificed by cervical dislocation and the tissue samples, including heart, liver, spleen, lung and kidney were immediately removed and washed with 0.9% saline solution; and then wiped using an absorbent paper, and the specimens were frozen at –20 °C until analysis.

After being recovered from deep freezer, 1 g of tissue samples were homogenized with 3 ml of normal saline, and 3 ml of homogenate were mixed with 3 ml of acetonitrile by vortex-mixing (XW-80A, Shanghai Medical University Instrument Factory, Shanghai, China) for 3 min. 1 ml of serum samples were vortexed with 1 ml of acetonitrile for 1 min as well. After centrifugation at 10,000 rpm for 10 min, the supernatant of tissue or serum samples were collected and evaporated under a nitrogen gas stream. The residues were vortexed with 200 μl of mobile phase and then filtered with 0.22 μm filter membrane. 20 μl of sample solution was injected into the HPLC system to detect the content of VBL in tissue and serum samples.

The HPLC system (1200, Agilent, USA) was equipped with a reverse-phase C18 column (Agilent, 250 × 4.60 mm, 5 μm) and ultraviolet-visible detector at the detection wavelength of 269 nm. 1.4% (v/v) triethylamine aqueous was adjusted to pH7.2 with phosphoric acid and used as mobile phase with acetonitrile (40:60, v/v). The flow rate was 1.0 ml/min at ambient temperature.

3. Results and discussion

3.1. *Optimization of MINPs synthesis*

According to the synthesis principle of MINPs and the result of preliminary experiments, four parameters, the moles of MAA (X_1), the moles of TRIM (X_2), the volumes of acetonitrile (X_3), and the reaction temperature (X_4) were selected as independent variables and the entrapment efficacy (Y) as the dependent variable. U_{10} ($10^2 \times 5^2$) uniform design (Table 1) was applied to optimize the MINPs process parameters. The investigated parameters were graded into ten or five levels and incorporated into ten trials with. Each trial was performed in triplicate.

As shown in Table 1, the entrapment efficacy of developed MINPs was in the range of 9.90 ± 0.24% to 76.60 ± 2.06% with different variable combinations. The best trial was MINPs 4, where the entrapment efficacy was 76.60 ± 2.06%.

DPS data processing system (V7.05 version) was adopted for the stepwise regression analysis of the experimental data, and the effect of independent variables on entrapment efficiency was proposed by the following polynomial equation:

$$Y_1 = 36.7568 + 112.0695X_1 - 93.6307X_2 + 0.5636X_3 - 73.3381X_1^2 + 32.2976X_2^2 \quad (4)$$

The equation would have maximal output when X_1 was 0.756 mmol, X_2 was 0.224 mmol, X_3 was 34.9 ml and X_4 was 59.9 °C. And the maximal predicted values of responses Y was 81.07% in the model.

To validate the result of Eq. (4), the optimized formulation (X_1 0.756 mmol, X_2 0.224 mmol, X_3 40 ml, and X_4 60 °C) was developed to synthesize MINPs and then characterized for entrapment efficacy. The experimental value for responses Y that is 83.25% of optimized formulation was found in good agreement with the predicted values generated by the stepwise regression Eq. (4). And the drug loading capacity of the optimal MINPs-VBL was 8.72%.

3.2. *EE% of MINPs with different concentration of VBL and adsorption time*

According to the preliminary experiments, we found the VBL loading efficiency would vary with different concentration of the VBL solution or different adsorption time. Hence, MINPs 4 and MINPs 5 were used to investigate the influence of different concentration of VBL solution (0.60 mmol/l, 1.25 mmol/l, 1.50 mmol/l, 3.00 mmol/l, 4.00 mmol/l, 8.00 mmol/l) and different incubating time (1 h, 2 h, 4 h, 7 h, 10 h, 15 h, 17 h, 19 h, 21 h, 23 h, 24 h) on the encapsulation efficiency (EE%) of VBL. As shown in Fig. 1A, the EE% of VBL was highest when incubated with VBL solution at the concentration of 1.25 mmol/l and then decreased gradually with the increase of VBL concentration. From Fig. 1B, we found that the EE% of VBL significantly increased when the incubating time extended and the value reached top at 4 h, after which it declined slightly. As a result, MINPs-VBL was prepared with 1.25 mmol/l of VBL solution oscillated with MINPs for 4 h.

3.3. *Morphology and particle size of MINPs*

Scanning electron microscopy (SEM) (HITACHI S-3000 SEM, Japan) was employed to determine the shape and surface morphology of the polymer particles made by the optimized formulation. The image from the SEM showed that MINPs were spherical particles with smooth surface and good dispersity (see Fig. 2).

The particle size and size distribution were measured by dynamic light scattering (DLS) (Malvern Zetasizer ZS, Malvern, UK). It showed that the particle size of MINPs was 300 ~ 450 nm (see Fig. 3).

3.4. *In vitro release of VBL from MINPs-VBL*

The *in vitro* release study of VBL from MINPs-VBL was performed in PBS (pH 7.4) at 37 °C (see Fig. 4). Quick release occurred in the initial 24 h, which could be related to the release of the drug adsorbed or precipitating on the surface of MINPs. In this phase, VBL released from MINPs-VBL with a process of solution–diffusion or desorption, and the amount was 19.49 ± 2.75%. Thereafter, the release rate became slow, demonstrating a typical behavior of sustained and prolonged drug release. It was due to the non-covalent interactions between

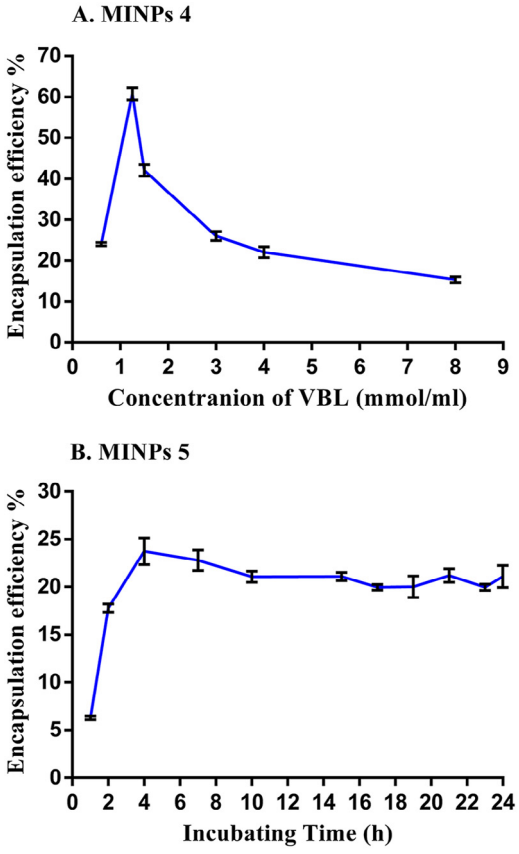

Fig. 1 – The influence of (A) different concentration of VBL and (B) adsorption time on EE% of MINPs.

model drug and MINPs, which delayed the release of the drug from the nanoparticles network. From 144 h on, the drug release further slowed down. The cumulative release percentage reached 71.45 ± 2.56% at 216 h. The drug entrapped deep inside the pores of MINPs needed to eliminate the non-covalent interactions and then passed much longer distance.

The *in vitro* release behavior was fitted using different release dynamic models (see Table 2). From Table 2, the *in vitro* drug-release kinetic model of MINPs-VBL fitted well with the first-order dynamic equation due to the maximum value of "r" (0.9942) and the minimum value of "AIC" (53.1998). The fitting curve of calculated release of MINPs-VBL was also shown in Fig. 4. We found the observed curve highly fitted with the calculated one, demonstrating that release of VBL from MINPs-VBL may be based on the solution–diffusion and desorption process.

The imprints on MINPs showed high selectivity and affinity to the template VBL, and could adsorb VBL steadily via the non-covalent bond including hydrogen bonding, electrostatic effect, etc. Therefore, we observed the sustained release of VBL from MINPs. Not only diffusion but also the adsorption between MINPs and VBL contributed to the drug releasing process of MINPs-VBL.

3.5. *Bio-distribution study*

To investigate the tissue distribution of MINPs-VBL and VBL injection, each formulation at a dosage of 5 mg/kg of VBL was injected by cauda vein to rats, and the samples were collected after 60 min.

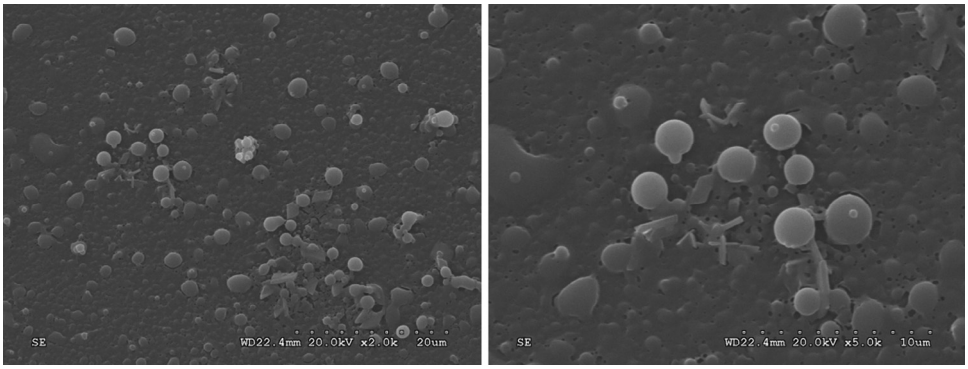

Fig. 2 – Scanning electron micrographs of MINPs.

From Fig. 5, it can be seen that for VBL injection group, the level of VBL was highest in heart (12.08 ± 0.24 μg/ml), followed by kidney, liver, spleen, lung, and lowest in serum. For MINPs-VBL group, the highest one was that in liver (52.02 ± 0.48 μg/ml), followed by kidney, heart, lung, spleen, and serum in that order. It was amazing that a significant increase of VBL concentration in MINPs-VBL group was observed compared to VBL injection group. Furthermore, 33% of VBL was distributed in liver in MINPs-VBL group but about 21% in VBL injection group. It indicated that the tissue distribution of VBL encapsulated in MINPs in rats was significantly altered in comparison with VBL injection, especially in liver.

To evaluate the drug targeting effect of MINPs-VBL *in vivo*, drug targeting index (DTI) and drug selecting index (DSI) were introduced and calculated by the following equations, and the results were shown in Table 3.

Compared with the VBL injection group, the drug level of MINPs-VBL was 5.29-fold in liver, 3.04-fold in lung, 2.93-fold in kidney and about 2.55-fold both in heart and in spleen. Although the VBL level of serum was the lowest in both groups, it was 3.81-fold in MINPs-VBL to that of in VBL injection group. It suggested that the sustained-release property of MINPs contributed to the higher drug levels of MINPs-VBL in tissues and serum. Comparing the levels of VBL in tissues with that of in serum, MINPs-VBL also showed obvious selectivity to liver relative to other tissues (see Table 3). That meant VBL in MINPs-VBL had higher affinity to liver tissue. It might have arisen from the mononuclear macrophage phagocytosis to MINPs-VBL particles, which were with the hydrophobic surface and being the sizes more than 200 nm, and the enrichment in tissues with rich reticulo endothelial system (RES), like liver etc. [12].

$$\text{DTI} = \frac{\text{The drug concentration in } A \text{ tissue of targeting preparation at } I \text{ time}}{\text{The drug concentration in } A \text{ tissue of non-targeting preparation at } I \text{ time}} \tag{5}$$

$$\text{DSI} = \frac{\textit{The drug concentration in A tissue at I time}}{\textit{The drug concentration in serum or non-targeting tissue at I time}} \tag{6}$$

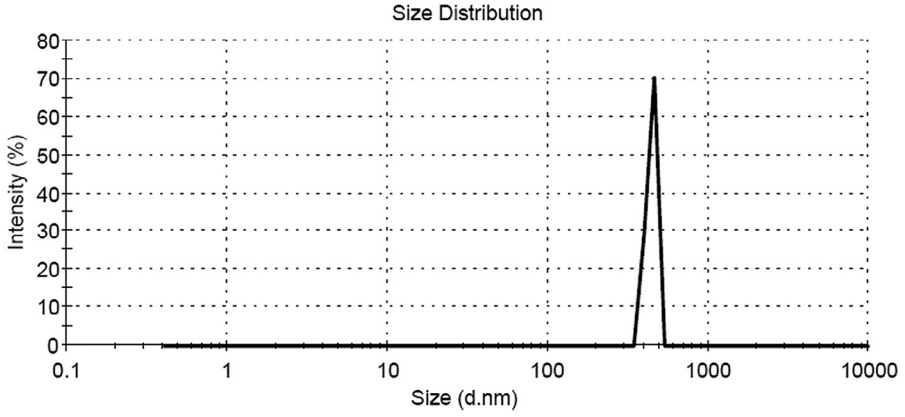

Fig. 3 – Particle size distribution of MINPs.

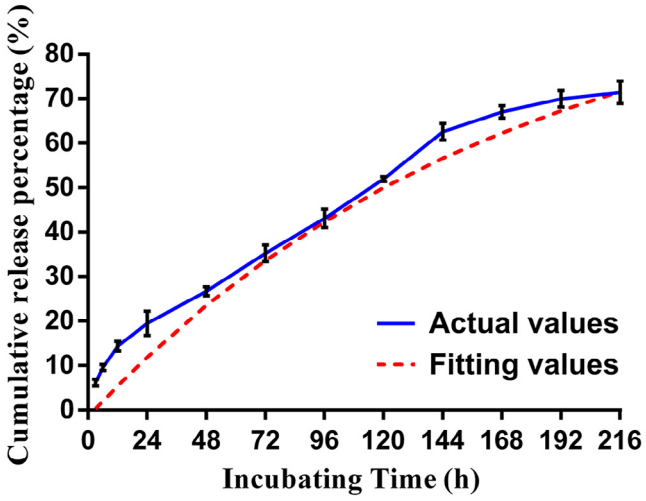

Fig. 4 – The *in vitro* release profile of MINPs-VBL.

4. Conclusion

The MINPs bearing cavities, complementary to the template molecule VBL, could absorb VBL via non-covalent interactions, such as hydrogen bonds, ionic bonds and hydrophobic effect, which provided MINPs with extraordinary release property as drug carriers. In this paper, we demonstrated that VBL loaded MINPs showed a sustained-release behavior *in vitro* that fitted well with the first-order kinetics model. And the drug level of VBL loaded MINPs in tissues and serum of SD rats was evidently higher than that of commercially available injection, especially in liver. It implied that the MINPs might be a potential sustained-release drug carrier and exhibited liver target to a certain extent. The biocompatibility of MINPs needed further study.

Table 2 – *In vitro* drug-release kinetic model of MINPs-VBL.

Fitting method	Fitting equation	r	AIC
Zero-order dynamic equation	Q = 0.3184t + 10.495	0.9879	74.76861
First-order dynamic equation	ln[1 – Q] = –0.0059t + 4.62	0.9942	53.1998
Higuchi equation	$Q = -3.0658 + 5.0808t^{1/2}$	0.9906	63.8489
Retger-peppas equation	lnQ(t) = 0.4981lnt + 1.5266	0.9850	73.79749

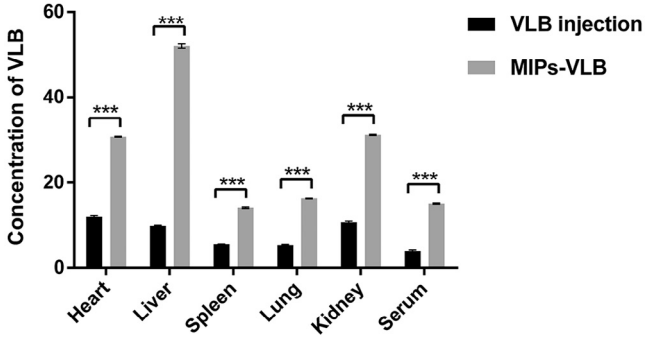

Fig. 5 – Concentration of VBL in serum and different tissues of rats after tail i.v. of MINPs-VBL and VBL injection (n = 6).

Table 3 – DTI and DSI of tissues after administrating MINPs-VBL and VBL injection by cauda vein at 60 min.

	Groups	Heart	Liver	Spleen	Lung	Kidney	Serum
DTI	MINPs-VBL	2.55	5.29	2.57	3.04	2.93	3.81
	VBL injection	1	1	1	1	1	1
DSI	MINPs-VBL	2.05	3.46	0.93	1.23	2.08	1
	VBL injection	3.06	2.50	1.40	1.58	2.70	1

Acknowledgments

This work was supported by the National Natural Science Foundation of China (grant number: 81173566).

REFERENCES

[1] Vasapollo G, Sole RD, Mergola L, et al. Molecularly imprinted polymers: present and future prospective. Int J Mol Sci 2011;12:5908–5945.
[2] Luliński P. Molecularly imprinted polymers: as the future drug delivery devices. Acta Pol Pharm 2013;70(4):601–609.
[3] Tse Sum Bui B, Haupt K. Molecularly imprinted polymers: synthetic receptors in bioanalysis. Anal Bioanal Chem 2010;398(6):2481–2492.
[4] van Nostrum CF. Molecular imprinting: a new tool for drug innovation. Drug Discov Today Technol 2005;2(1):119–124.
[5] Asadi E, Azodi-Deilami S, Abdouss M, et al. Cyproterone synthesis, recognition and controlled release by molecularly imprinted nanoparticle. Appl Biochem Biotechnol 2012;167(7):2076–2087.
[6] Abdouss M, Asadi E, Azodi-Deilami S, et al. Development and characterization of molecularly imprinted polymers for controlled release of citalopram. J Mater Sci Mater Med 2011;22(10):2273–2281.
[7] Jantarat C, Tangthong N, Songkro S, et al. S-propranolol imprinted polymer nanoparticle-on-microsphere composite porous cellulose membrane for the enantioselectively controlled delivery of racemic propranolol. Int J Pharm 2008;349(1–2):212–225.
[8] Marinina J, Shenderova A, Mallery SR, et al. Stabilization of vinca alkaloids encapsulated in poly(lactide-co-glycolide) microspheres. Pharm Res 2000;17(6):677–683.
[9] Zu Y, Zhang Y, Zhao X, et al. Optimization of the preparation process of vinblastine sulfate (VBLS)-loaded folate-conjugated bovine serum albumin (BSA) nanoparticles for tumor-targeted drug delivery using response surface methodology (RSM). Int J Nanomedicine 2009;4:321–333.
[10] Zhigaltsev IV, Maurer N, Akhong QF, et al. Liposome-encapsulated vincristine, vinblastine and vinorelbine:

a comparative study of drug loading and retention. J Control Release 2005;104(1):103–111.
[11] Prabu P, Chaudhari AA, Dharmaraj N, et al. Preparation, characterization, in-vitro drug release and cellular uptake of poly(caprolactone) grafted dextran copolymeric nanoparticles loaded with anticancer drug. J Biomed Mater Res A 2009;90(4):1128–1136.
[12] Gupta AK, Gupta M. Synthesis and surface engineering of iron oxide nanoparticles for biomedical applications. Biomaterials 2005;26(18):3995–4021.